Analysis of a Model for Excitation of Myelinated Nerve

DONALD R. McNEAL, MEMBER, IEEE

Abstract—**Excellent models have been presented in the literature which relate membrane potential to transverse membrane current and which describe the propagation of action potentials along the axon, for both myelinated and nonmyelinated fibers. There is not, however, an adequate model for nerve excitation which allows one to compute the threshold of a nerve fiber for pulses of finite duration using electrodes that are not in direct contact with the fiber. This paper considers this problem and presents a model of the electrical properties of myelinated nerve which describes the time course of events following stimulus application up to the initiation of the action potential. The time-varying current and potential at all nodes can be computed from the model, and the strength-duration curve can be determined for arbitrary electrode geometries, although only the case of a monopolar electrode is considered in this paper. It is shown that even when the stimulus is a constant-current pulse, the membrane current at the nodes varies considerably with time. The strength-duration curve calculated from the model is consistent with previously published experimental data, and the model provides a quantitative relationship between threshold and fiber diameter which shows there is less selectivity among fibers of large diameter than those of small diameter.**

INTRODUCTION

INTEREST in the clinical application of electrical stimulation of nerves, both peripherally and centrally, is growing rapidly. Thousands of patients are now being treated for chronic pain using both superficial and implanted electrodes [1], [2]. Glenn *et al.* [3] have developed an electrophrenic respirator which has been implanted in nearly 100 patients with inadequate or no respiratory function. Waters *et al.* [4] have reported on a series of stroke victims in which paralyzed muscles of the leg are activated electrically during ambulation to improve walking. Experimental work is underway to develop neuroelectric prostheses for the deaf and blind [5], [6]. As these clinical efforts multiply, it becomes imperative that a model of nerve stimulation be available to provide an analytical foundation for the design of electrodes for these and future applications.

FitzHugh [7] and Pickard [8] analyzed the propagation of an action potential along a myelinated nerve fiber by modeling the myelin sheath as a distributed leaky capacitance and by assuming the nodal membrane obeyed the equations of Hodgkin and Huxley for a squid axon [9]. A similar model was used by Goldman and Albus to theoretically establish a linear relationship between conduction velocity and fiber diameter [10]. They modeled the nodal membrane by using equations empirically derived by Frankenhaeuser and Huxley for myelinated frog nerve [11]. In each of these analyses, excitation was assumed to be initiated by a stimulus current applied at one of the nodes. This is a valid assumption when the stimulus is applied through a microelectrode, but it is not sufficient for the case of macroelectrodes, where the simulus produces currents at many nodes simultaneously.

Rushton was the first to theoretically calculate the threshold of a nerve for a specific electrode geometry [12]. He considered the case of bipolar electrodes in contact with a nonmyelinated nerve, and derived a curve relating threshold to the spacing between electrodes that provided an excellent match with experimental data. This paper and subsequent publications (e.g., Rushton, 1934, 1937) have provided a basis for much of the analytical work on nerve excitation up to the present [13], [14]. For instance, Lale used a similar, though simplified, approach to calculate threshold for muscle stimulation [15]. Noble used Rushton's concept of "liminal length" to derive a theoretical strength-duration curve for Purkinje fibers [16]. Rushton's contribution is quite remarkable considering that, at the time of his first publication, a theory that the excitable structures of the nerve were a series of transverse membranes within the fiber was still being given serious consideration.

Excitation of myelinated fiber was specifically considered by Lussier and Rushton [17]. They obtained an analytical solution for threshold, but their solution was again limited to the case of bipolar electrodes which were assumed to be in direct contact with the nerve. BeMent and Ranck were interested in the relationship between the threshold of a myelinated nerve and the distance of a monopolar electrode from a node [18]. They obtained a solution for the special case of a spherical electrode located directly above one of the nodes. A more general solution was obtained by Bean in an Appendix of Abzug *et al.* [19]. He derived a closed-form solution that is valid when the electrode is close to a node and an iterative solution for arbitrary locations.

In each of the papers cited in the previous two paragraphs, only steady-state conditions were considered; i.e., threshold is determined only for a pulse of infinite duration. Thresholds for finite duration pulses must then be obtained by reference to an experimentally determined strength-duration curve. The purpose of this paper is to present and analyze a model for the electrical properties of a myelinated nerve fiber that allows the computation of strength-duration curves for arbitrary electrode configurations. In addition, the time-varying transverse membrane current and membrane potential at each of the nodes of Ranvier are determinable from the model for subthreshold stimuli and for suprathreshold stimuli up to the time of initiation of the action potential.

The emphasis in this paper will be on a detailed presentation and discussion of the model as well as a thorough examination of the transient response for the special case of a monopolar

Manuscript received October 27, 1975; revised February 15, 1976. This project was supported in part by the Rehabilitation Services Administration of the Department of Health, Education, and Welfare under Grant 23-P-55442/9-04.

The author is with the Rehabilitation Engineering Center, Rancho Los Amigos Hospital, University of Southern California, Downey, CA 90242.

spherical electrode located directly over and 1 mm away from one of the nodes. A consideration of other electrode geometries is left for future analysis. Only monophasic, constant-current pulses are considered. Subthreshold responses are presented, a strength-duration curve is calculated and the effect of fiber diameter on threshold is examined.

General Theory

A myelinated nerve fiber can be approximated by the equivalent electrical network shown in Fig. 1. Symbols for variables and constants and the values of constants used in this paper are given in Table I. The assumptions generally follow those of FitzHugh [7], except that it is assumed here that the myelin sheath is a perfect insulator. The validity and effect of this assumption is considered later in the Discussion section. Following FitzHugh, it is assumed that the fiber is infinitely long with nodes that are regularly spaced. Both internodal distance and axon diameter are assumed to be proportional to fiber diameter. The nodal gap width is considered to be a constant for all fiber diameters which implies that the nodal membrane area is also proportional to fiber diameter. This is consistent with the theoretical predictions of Rushton [20] and Dun [21]. In addition to FitzHugh, the reader is referred to Goldman and Albus [10] for a review of the experimental evidence supporting the above assumptions.

The internodal conductance G_a can be calculated from

$$G_a = \pi d^2/4\rho_i L. \tag{1}$$

The membrane impedance is represented by a capacitor C_m and conductance G_m in parallel which are given by

$$G_m = g_m \pi dl \tag{2}$$

and

$$C_m = c_m \pi dl. \tag{3}$$

Note that all three of these components are proportional to fiber diameter. ($G_a \propto d$ since $L \propto d$. See previous paragraph.) For a given diameter, G_a and C_m are constants, but G_m is, in general, a complex function of the membrane potential.

This model assumes that the electrical potential outside the fiber is determined only by the stimulus current, tissue outside the nerve fiber and the electrode geometry, and is not distorted by the presence of the fiber. This is reasonable since the dimensions of a single nerve fiber are small and because our interest is limited to the period of time prior to excitation (before internally generated currents become significant). The small dimensions of the fiber also allow the simplification that the external surface of the membrane at any one node is at an equipotential. This implies that variations in the membrane current density over the nodal surface can be neglected. These assumptions are considered further in the Discussion section.

In this paper, it will be assumed that the medium external to the nerve fiber is infinite and isotropic. This assumption is not vital to the model, and both anisotropic and finite external mediums can be considered. Calculation of the potential throughout the medium, of course, becomes more complex as more realistic models for the external environment are formulated.

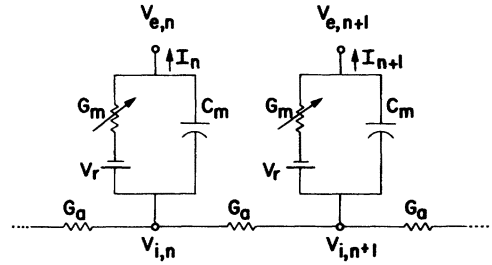

Fig. 1. Electrical network representation of a myelinated nerve fiber.

TABLE I
Variables and Constants

Variables		
t		time (microseconds)
V_n		membrane potential at node n minus the resting potential (millivolts)
I_n		membrane current at node n (pa)
$V_{e,n}$		external potential at node n
$V_{i,n}$		internal potential at node n
G_a		axial internodal conductance
G_m		nodal membrane conductance
C_m		nodal capacitance
D		fiber diameter (external myelin diameter)
d		axon diameter (internal myelin diameter)
L		internode length
$I_{i,n}$		total ionic current at node n
i_{Na}		sodium current density
i_K		potassium current density
i_P		nonspecific delayed current density
i_L		leak current density
I		stimulus current
T		stimulus duration
Constants		
ρ_i	110 Ω · cm	axoplasm resistivity (Stampfli [25])
ρ_e	300 Ω · cm	resistivity of external medium (Abzug *et al.* [19])
c_m	2 μF/cm^2	membrane capacitance/unit area (Frankenhaeuser and Huxley [11])
g_m	30.4 mmho/cm^2	membrane conductance/unit area (Frankenhaeuser and Huxley [11])
l	2.5 μm	nodal gap width (Dodge and (Frankenhaeuser [26])
L/D	100	ratio of internodal space to fiber diameter (Hursh [27] and Dodge and Frankenhaeuser [26])
d/D	0.7	ratio of axon and fiber diameters (Goldman and Albus [10])
V_r	-70 mV	resting potential (Frankenhaeuser and Huxley [11])

The membrane current at node n is equal to the sum of the incoming axial currents and to the sum of the capacitive and ionic currents through the membrane. Hence,

$$C_m \frac{dV_n}{dt} + I_{i,n} = G_a(V_{i,n-1} - 2V_{i,n} + V_{i,n+1}). \tag{4}$$

For subthreshold stimuli, it can be assumed that the membrane conductance is constant. (See Discussion.) The ionic current at node n is then given by $G_m V_n$. Substituting this into (4), it can be shown that the myelinated fiber is described by the following infinite set of linear, first-order differential equations:

$$\frac{dV_n}{dt} = \frac{1}{C_m}[G_a(V_{n-1} - 2V_n + V_{n+1} + V_{e,n-1} - 2V_{e,n} + V_{e,n+1}) - G_m V_n]$$
$$(n = \cdots -2, -1, 0, 1, 2, \cdots) \quad (5)$$

where V_n is given by $V_{i,n} - V_{e,n} - V_r$. The initial conditions are simply

$$V_n(0) = 0 \quad \text{for all } n \quad (6)$$

because of the capacitance C_m shunting each node.

An approximate solution to (5) and (6) can be obtained by selecting a finite set of differential equations that enclose the nodes of interest and then integrating the finite set to obtain the membrane potentials. If the set of differential equations is large enough, it can safely be assumed that the membrane potential at the boundary nodes and at all nodes outside the selected set is zero. For the electrode geometry considered in this paper, it was found that a set of eleven first-order equations, including the node below the electrode and five adjacent nodes on each side, yielded a membrane potential at the node below the electrode that was accurate to better than 0.2 percent throughout a 1 ms pulse. This was determined by comparing the solution for eleven nodes with solutions for 21 and 31 nodes.

The node at which excitation will initially occur can be predicted from the subthreshold response. Excitation will occur at the node at which the membrane potential is a maximum during the time of stimulus application. This node will be referred to as the excitation node. As the stimulus is increased to threshold or suprathreshold values, the membrane conductance at the excitation node changes markedly during the stimulus as the membrane becomes more permeable to sodium ions. A much more accurate representation of the membrane potential can be obtained by assuming that the membrane at the excitation node is modeled by the Frankenhaeuser-Huxley equations for the membrane of a myelinated frog fiber [11]. It can still be assumed that the membrane conductance at all other nodes is constant since the membrane potential at these nodes will be subthreshold prior to the initiation of an action potential at the excitation node. This is a satisfactory assumption since our interest, in this paper, is confined to 1) determining whether an action potential is initiated and 2) calculating the transient response for subthreshold stimuli and for suprathreshold stimuli up to the time an action potential is initiated. There will be certain cases (e.g., a monopolar electrode located exactly between two nodes) where the maximum depolarization is the same or nearly the same at two or more nodes. Under these conditions, the membrane at each of these nodes would have to be modeled by the Frankenhaeuser-Huxley equations. The following equations are written for the case where only one node is significantly depolarized, but the extension to two or more nodes is straightforward.

For stimuli near or greater than threshold, the ionic current at the excitation node (assumed to be node 0) is given by

$$I_{i,0} = \pi dl(i_{Na} + i_K + i_P + i_L) \quad (7)$$

where the terms on the right are the individual components of ionic current (expressed as current densities) specified by Frankenhaeuser and Huxley [11]. For the reader's convenience, the equations for these terms are given in the Appendix. The complete set of equations describing the time course of the membrane potential at all nodes prior to excitation is now given by

$$\frac{dV_n}{dt} = \frac{1}{C_m}[G_a(V_{n-1} - 2V_n + V_{n+1} + V_{e,n-1} - 2V_{e,n} + V_{e,n+1}) - G_m V_n] \quad \text{for } n \neq 0 \quad (8)$$

$$\frac{dV_0}{dt} = \frac{1}{C_m}[G_a(V_{-1} - 2V_0 + V_1 + V_{e,-1} - 2V_{e,0} + V_{e,1}) - \pi dl(i_{Na} + i_K + i_L + i_P)] \quad (9)$$

$$V_n(0) = 0 \quad \text{for all } n. \quad (10)$$

Equations (8)-(10) can be solved by integrating a finite set of equations as described previously for the subthreshold case.

Calculation of the external potential at each node is easy for the case considered in this paper. For a monopolar spherical electrode in an isotropic medium, the electrical potential at a distance r from the electrode is simply

$$V_e = \frac{\rho_e I}{4\pi r}. \quad (11)$$

Current flowing toward the electrode is considered to be positive. Once the location of the electrode with respect to the nerve has been established, it is straightforward to calculate the potential at each node using (11). Note that the external potential is time-invariant when the stimulus current is constant, as in this example. This is a convenient, but not necessary simplification to this model. Because of the assumed symmetry of the electrode geometry considered in this paper, the external potential at nodes n and $-n$ is equal for all $n \neq 0$, which implies that the membrane potential and current at nodes n and $-n$ will be identical.

Other electrode geometries and more realistic external mediums can be considered. For example, multipolar spherical electrodes are easily considered by linear superposition of terms like the right-hand side of (11). Anisotropies of the external medium can be considered with little additional complexity [18]. Finite external mediums, electrodes of more complex shape and insulating surfaces can also be considered, but this will in general require a solution of Green's function with appropriate boundary conditions.

Results

Subthreshold Response

The subthreshold response of a 20 μm diameter fiber to a 0.1 mA pulse of infinite duration, calculated from (5) and (6), is shown in Figs. 2 and 3. (All of the results presented in this paper are for a 20 μm fiber except for those shown in Fig. 8 where the effect of fiber diameter on threshold is specifically considered.) Fig. 2 shows the change in membrane potential at the node below the electrode and at the four adjacent nodes. Initially, only node 0 is depolarized; however, nodes 1 and -1 reverse sign at 70 μs and remain depolarized from that time on.

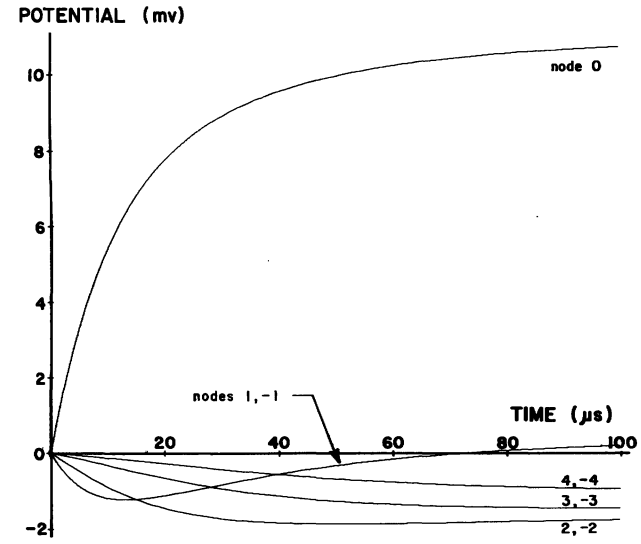

Fig. 2. Membrane potential at node beneath cathode (node 0) and adjacent nodes in response to a 0.1 mA monophasic, constant-current stimulus through a monopolar electrode placed 1 mm from the fiber. (Fiber diameter, 20 μm; internodal spacing, 2 mm.)

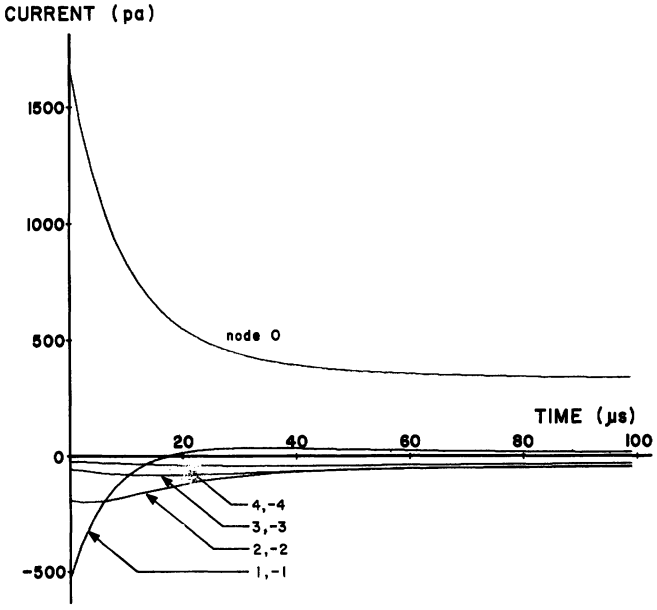

Fig. 3. Membrane current at node beneath cathode (node 0) and adjacent nodes in response to a 0.1 mA monophasic, constant-current stimulus through a monopolar electrode placed 1 mm from the fiber. (Fiber diameter, 20 μm; internodal spacing, 2 mm.)

All other nodes are hyperpolarized. For anodal stimulation, the signs of all curves are reversed, and it is seen that the site of initial excitation shifts from nodes 1 and -1 for pulse durations less than 15 μs to nodes 2 and -2 for longer pulse durations.

The time response of the membrane current at these same nodes is shown in Fig. 3. Membrane current from inside to outside is taken to be positive. The most striking feature of these curves is the rapidity with which membrane current at node 0 falls off with time even though the stimulus current is constant at 0.1 mA. At 20 μs, the membrane current at node 0 has fallen to one-third of the initial value and continues to fall to a steady-state value that is approximately one-fifth of the initial value. Most of the initial current is capacitive, but the ionic component dominates for $t > 50$ μs. Currents at nodes 1 and -1 are initially negative, but become positive after 20 μs accounting for the eventual reversal of membrane potential at these nodes. Membrane current is negative at all other nodes.

The response at node 0 to a monophasic 0.1 mA pulse of 100 μs duration is shown in Fig. 4. At the termination of the pulse, the change in membrane current is equal and opposite to the change at $t = 0$. A significant negative current, therefore, flows after the stimulus has been terminated. For the case shown, the negative charge crossing the membrane after the pulse is terminated is nearly one-third of the total positive charge crossing the membrane during the pulse. The ratio becomes even higher at shorter pulse durations, so the net charge crossing the membrane is significantly less than the positive charge that crosses during the pulse. The effect of this negative spike on the membrane potential is to drive the potential back to zero very rapidly. It is interesting to note that the average total current flowing through the nerve during a 100 μs pulse is less than 5/1 000 000 of the applied stimulus current even though the electrode is only 1 mm from the nerve.

Threshold Response

It is seen from Fig. 2 that excitation will initially occur at node 0. (Of course, in this case, the observation is not surprising. With more complex electrode geometries, it is not always obvious at which node excitation will occur.) A more accurate response near threshold can now be obtained by using (8)-(10). The change in membrane potential at node 0 for a 100 μs pulse is shown in Fig. 5. Threshold is 0.226 mA. Response to three amplitudes of stimulus current are shown: 0.220, 0.225, and 0.230 mA. The action potential initiated by the 0.230 mA stimulus is not shown in the figure in order to concentrate on the response prior to excitation. As threshold is approached, the membrane conductance G_m begins to change, slowly at first, and then more rapidly as the membrane permeability to sodium ions increases. This accounts for the upward bend in the potential response toward the end of the pulse. The negative dip following pulse termination, seen even in the suprathreshold response (0.230 mA), is accentuated by the negative current spike seen in Fig. 4(a).

Threshold responses for pulse durations of 10, 100, and 1000 μs (up to the initiation of the action potential) are shown in Fig. 6. The time axis is normalized by the pulse duration so that the transient response is more apparent in each case. It is clearly shown that there is not a critical potential at which threshold occurs for all pulse durations. For a pulse duration of 1000 μs the membrane potential prior to the initiation of the action potential is approximately 20 mV, whereas the potential must reach 58 mV before excitation occurs for a duration of 10 μs. The large potential change required at 10 μs is due primarily to the negative current spike at pulse termination. The effect of the negative current spike is to "turn off" the rapid changes in membrane permeability that produce the action potential, and this effect is most prominent at the shorter pulse duration. If the membrane current in the Frankenhaeuser-Huxley equations is set to zero following a positive

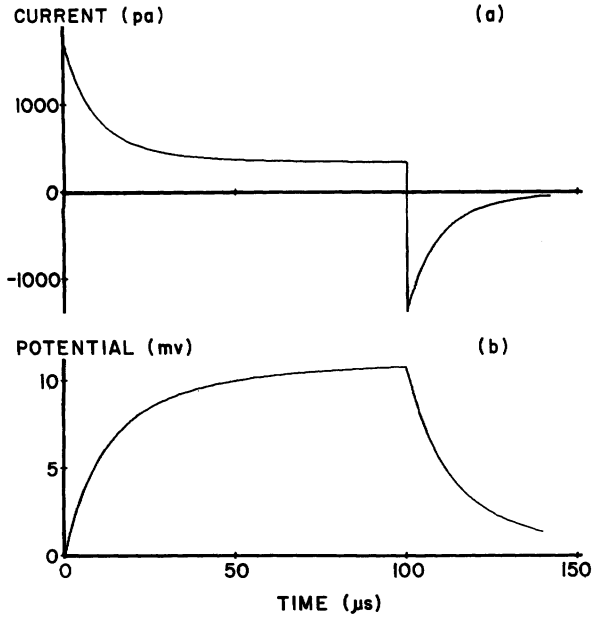

Fig. 4. Membrane current (a) and potential (b) at node beneath cathode in response to a 0.1 mA monophasic, constant-current pulse of 100 μs duration.

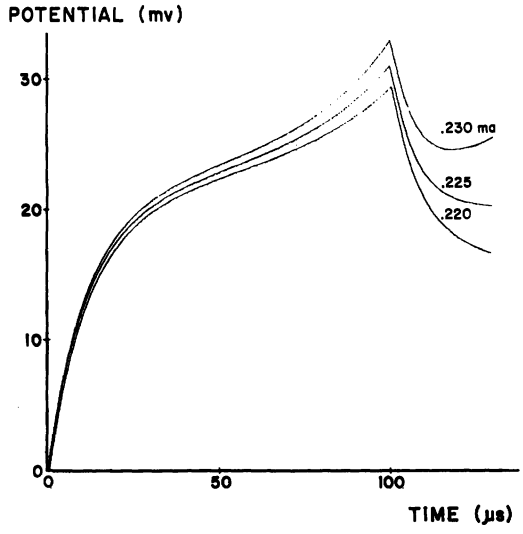

Fig. 5. Membrane potential at node beneath cathode above threshold (0.23 mA) and near threshold (0.225 and 0.22 mA) for a 100 μs pulse duration. Threshold is 0.226 mA.

current pulse, the membrane potential at threshold never exceeds 30 mV during stimulus application.

The strength-duration curve calculated over the range of 10-1000 μs is shown in Fig. 7. Chronaxie is approximately 80 μs. It is interesting to note that the slope, even at short pulse durations, does not equal -1, which would be the case if the stimulus charge was constant at short pulse durations. This means that the stimulus charge at threshold continues to decrease with decreasing pulse duration—even as low as 10 μs.

Effect of Fiber Diameter

All of the previous results were calculated for a 20 μm diameter fiber. The purpose of this section is to consider the effect of fiber diameter on threshold. Examining (8) and (9), the

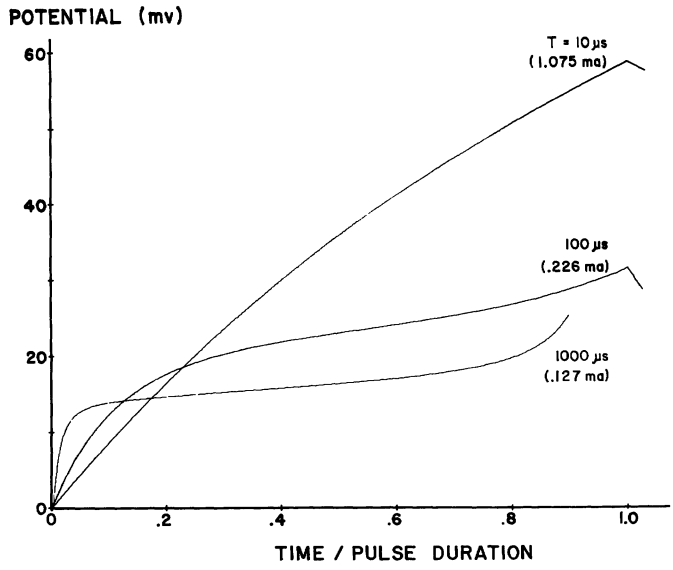

Fig. 6. Membrane potential at node beneath cathode at threshold durations of 10, 100, and 1000 μs. Abscissa is normalized by pulse duration to better illustrate the transient response. Threshold current is given in parentheses.

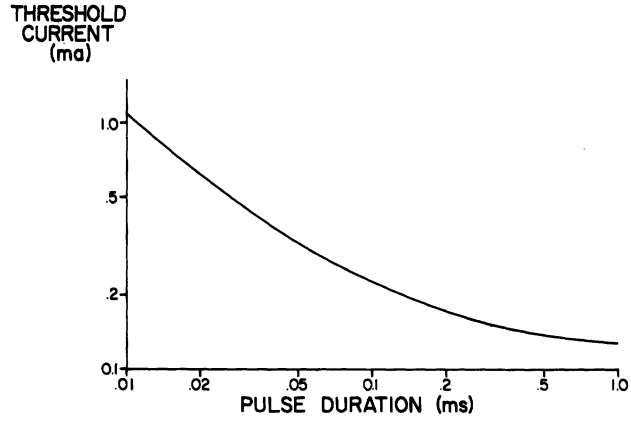

Fig. 7. Strength-duration curve for a 20 μm fiber (internodal spacing, 2 mm) with a monopolar electrode located 1 mm above one of the nodes.

terms that are functions of fiber diameter are C_m, G_a, G_m, πdl, and the external potentials. The first four terms, as pointed out previously, are proportional to fiber diameter. However, they occur only in (8) and (9) as ratios (e.g., G_a/C_m), so the ratios are independent of fiber diameter. The only effect then of changing fiber diameter is in the calculation of the external potential at the nodes. This will change (at all nodes other than node 0) because the internodal spacing is proportional to fiber diameter. As fiber diameter is changed, the distance of each node from the electrode is changed and the calculated potentials will be different.

Threshold current at a duration of 100 μs is plotted in Fig. 8 for fiber diameters ranging from 2 to 25 μm. As expected, threshold increases as fiber diameter is decreased. If threshold was inversely proportional to fiber diameter, the curve would be a straight line with a slope of -1. As seen in the figure, the slope at 25 μm is approximately $-\frac{1}{2}$ while the slope at 2 μm is nearly -2. Thus, at the larger diameters (>15 μm), threshold is approximately inversely proportional to the square root of

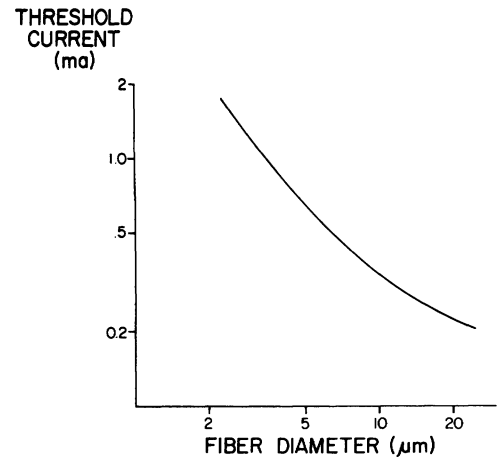

Fig. 8. Threshold current as a function of fiber diameter with a monopolar electrode located 1 mm above one of the nodes.

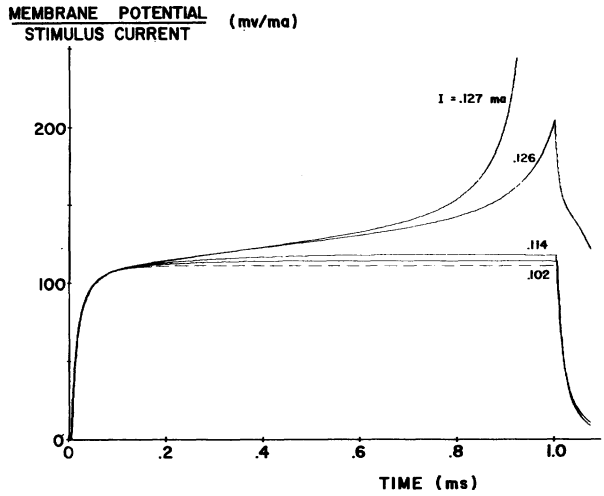

Fig. 9. Membrane potential at node beneath the cathode for a 1.0 ms monophasic, constant-current stimulus. The ordinate is normalized by the stimulus current. Threshold response (0.127 mA) is shown along with subthreshold responses of 0.126, 0.114, and 0.102 mA. The dashed line is the normalized potential assuming linearity (constant membrane conductance).

fiber diameter. In the small diameter range (<5 μm) threshold approaches an inverse square relationship with fiber diameter. This means that there will be less selectivity among fibers of different diameters in the larger diameter range than in the smaller diameter range.

Discussion

In the preceding analysis it has been assumed that 1) for subthreshold stimuli the membrane conductance is constant at all nodes and 2) near threshold the membrane conductance is constant at all nodes prior to the initiation of the action potential except at the excitation node where the membrane is modeled by the Frankenhaeuser-Huxley equations. The validity of this assumption will now be considered. The response at the excitation node to various stimulus amplitudes for a 1 ms pulse is shown in Fig. 9. For this case, threshold is 0.127 mA. Subthreshold responses for 0.126, 0.114, and 0.102 mA (prior to the action potential) are also shown, the last two being 90 and 80 percent of threshold. All responses are normalized by dividing the membrane potential by the stimulus current. If the membrane conductance is assumed to be constant at all nodes, then the normalized response for all stimulus amplitudes, because of system linearity, is given by the single dashed line in Fig. 9. The solid lines indicate the fiber response to the indicated stimulus amplitudes as predicted from (8)-(10) in which membrane conductance at the excitation node is allowed to vary as predicted by the Frankenhaeuser-Huxley equations. It is seen that as threshold is approached, the assumption of constant membrane conductance is no longer valid since the potential curves differ markedly from the linear response (dashed line). The assumption is quite good, however, for subthreshold stimuli that are 80 percent or less than threshold. At 80 percent of threshold, the response obtained by assuming that membrane conductance is constant is within 3 percent of that predicted by the more exact representation over the entire 1 ms period. The match is even better at lower stimulus levels. Similar results are obtained for shorter pulse durations.

The results of Fig. 9 demonstrate that the approximation of constant membrane conductance is valid for stimuli that are 80 percent of threshold or less. For near-threshold and suprathreshold stimuli, the membrane conductance at the excitation mode must be allowed to vary. The membrane conductance at all other nodes can still be considered to be constant since the membrane potential at these nodes remains low until the action potential begins to develop at the excitation node. As mentioned previously, there are cases where significant depolarization may occur at two or more nodes. The number of nodes at which G_m must be variable is easily determined from the subthreshold response. If the membrane potential at a node (say node j) is greater than 80 percent of the potential at the node of maximum depolarization, then the membrane conductance at node j must also be allowed to vary.

A second assumption made in the analysis is that the surface of each node is at an equipotential equal to $V_{e,n}$, which is defined to be the external potential at the point occupied by node n, but calculated by assuming the fiber is not present. There will of course be some variation in potential over the nodal surface due to the finite size of the fiber. This variation is not easily calculated because of the distortion of the external field in the neighborhood of the fiber; however, the variation in external potential over the nodal surface will not differ significantly from $V_{e,n}$—at least in comparison with the difference in potential between node n and its adjacent nodes. By a similar argument, the potential on the inner surface of node n will vary, but the variation will be small in comparison with the difference in internal potential between adjacent nodes. Therefore, the axial current flowing into node n and the total membrane current at node n will be approximately equal to $G_a(V_{i,n-1} - 2V_{i,n} + V_{i,n+1})$ as previously assumed in (4). This current will flow from node n with an approximately uniform distribution as previously assumed. There will be some distortion of this flow because of the external gradient due to the applied stimulus, but this will be a small effect.

A second component of current exists which has been neglected in this analysis. This is due to the current flowing

in the external medium when the stimulus is applied; e.g., in the example considered in this paper the current density at a distance of 1 mm from the monopolar electrode is 0.8 mA/cm^2 for a stimulus current of 0.1 mA. With the fiber present, some of this current will flow through node 0—entering on the far side and exiting on the near side. An exact calculation of this component would require a complex three-dimensional analysis, but an approximation to this term is obtained below by calculating the current flowing through an imaginary cylinder through node 0. [See Fig. 10(a).] Assume the cylinder is oriented so the axis of the cylinder is parallel to the current flow in the external medium. The impedance of the cylinder can be approximated by the electrical circuit shown in Fig. 10(b).

Assuming no distortion of the external field due to the presence of the fiber, it is easily shown from (11) that the far side of node 0 is 0.334 mV positive with respect to the near side and the current density through the cylinder due to this gradient is

$$j(t) = 2.164e^{-(t/0.22)} + 0.005. \tag{12}$$

From (12) it is seen that there is a significant component (2.164 mA/cm^2) due to the external gradient immediately after the stimulus is turned on. It is, in fact, larger than the uniform current density (calculated to be 1.51 mA/cm^2 from Fig. 3). It does not significantly affect the membrane potential, however, because the time constant of this component is only 0.22 μs, and the steady-state value of 0.005 mA/cm^2 is small in comparison with the steady-state value of the uniform current density (0.3 mA/cm^2, also calculated from Fig. 3). There is, of course, some distortion of the external field in the neighborhood of the fiber. This will affect the absolute values in (12), but the time constant which depends upon the assumed parameters of the fiber model should not be significantly affected. In summary, there will be significant skewing of the current distribution over the nodal surface immediately after stimulus application, but only during the first microsecond. After that, the assumption of uniform current density and the values of membrane current computed in this paper should be quite valid.

The most serious error in the model is introduced by the assumption that the myelin sheath is a perfect insulator, which it is not. Tasaki found the resistance and capacitance of the myelin sheath to be 290 M$\Omega \cdot$ mm and 1.6 $\mu\mu$F/mm, respectively [22]. The effect of current leaking through the myelin sheath on the results presented in this paper is difficult to assess without resorting to a much more complex simulation which would include sets of partial differential equations to describe the change in potential along the internodal regions as well as at the nodes. Due to the complexity of this simulation, this has not been done. Qualitatively, one can assume that the strength-duration curves presented in Fig. 7 would be shifted up slightly since all of the current will not pass through the nodes and the efficiency of stimulation will be somewhat decreased. How this shift will vary with pulse duration is difficult to predict.

Despite the error introduced by assuming that myelin is a perfect insulator, it is felt that the model presents an adequate representation of the myelinated fiber prior to excitation, and little additional insight would be gained by a more complex simulation. At the same time, much would be lost due to the enormous increase in computation time that the more complex model would require.

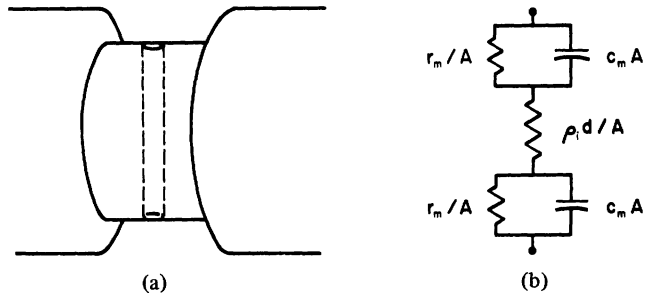

Fig. 10. (a) Schematic representation of imaginary cylinder through node 0. (b) Equivalent electrical circuit for the impedance of the cylinder where A is the area of the cylinder base.

Assumptions about values of nerve constants, relationships between diameters and internodal spacing, and the approximation of the membrane surface by the Frankenhaeuser-Huxley equations are based on the best information currently available on myelinated nerve. None of these assumptions appear to be critical to the model, and the model can be updated in the future as more precise data become available.

No attempt has yet been made to experimentally confirm the model, but the results presented in this paper appear to be consistent with available data. A chronaxie of 80 μs, found from the strength-duration curve in Fig. 8, compares favorably with data reported by BeMent and Ranck [23]. The finding that stimulus charge decreases with decreasing pulse duration—even down to 10 μs—is consistent with experimental data of Crago *et al.* [24]. The model also predicts an increase in threshold with decreasing fiber diameter, which is a well-known phenomenon. Unfortunately, there is a scarcity of experimental data available to compare with the computed curve.

Summary

A model for a myelinated nerve has been presented which allows threshold to be computed for arbitrary electrode configurations. In this paper, only the specific case of a monopolar spherical electrode located over a node at a distance of 1 mm is considered. Analysis of other electrode configurations will be the subject of a future paper. The time history of the membrane potential and membrane current at nodes close to the electrode are presented for threshold and subthreshold stimulation. The strength-duration curve is calculated, and a theoretical curve relating threshold to fiber diameter is presented.

Appendix

For the reader's convenience, the equations for the ionic components of transmembrane current for myelinated fiber as given by Frankenhaeuser and Huxley [11] are reported below.

$$i_{Na} = \bar{P}_{Na} hm^2 \frac{EF^2}{RT} \frac{(Na)_0 - (Na)_i e^{EF/RT}}{1 - e^{EF/RT}}$$

$$i_K = P'_K n^2 \frac{EF^2}{RT} \frac{(K)_0 - (K)_i e^{EF/RT}}{1 - e^{EF/RT}}$$

$$i_P = \bar{P}_P p^2 \frac{EF^2}{RT} \frac{(Na)_0 - (Na)_i e^{EF/RT}}{1 - e^{EF/RT}}$$

$$i_L = g_L(V - V_L)$$

where

$$E = V + V_r$$

$$dm/dt = \alpha_m(1 - m) - \beta_m m$$

$$dh/dt = \alpha_h(1 - h) - \beta_h h$$

$$dn/dt = \alpha_n(1 - n) - \beta_n n$$

$$dp/dt = \alpha_p(1 - p) - \beta_p p$$

and

$$\alpha_m = 0.36(V - 22)\left[1 - \exp\left(\frac{22 - V}{3}\right)\right]^{-1}$$

$$\beta_m = 0.4(13 - V)\left[1 - \exp\left(\frac{V - 13}{20}\right)\right]^{-1}$$

$$\alpha_h = 0.1(-10 - V)\left[1 - \exp\left(\frac{V + 10}{6}\right)\right]^{-1}$$

$$\beta_h = 4.5\left[1 + \exp\left(\frac{45 - V}{10}\right)\right]^{-1}$$

$$\alpha_n = 0.02(V - 35)\left[1 - \exp\left(\frac{35 - V}{10}\right)\right]^{-1}$$

$$\beta_n = 0.05(10 - V)\left[1 - \exp\left(\frac{V - 10}{10}\right)\right]^{-1}$$

$$\alpha_p = 0.006(V - 40)\left[1 - \exp\left(\frac{40 - V}{10}\right)\right]^{-1}$$

$$\beta_p = 0.09(-25 - V)\left[1 - \exp\left(\frac{V + 25}{20}\right)\right]^{-1}$$

Constants

$\bar{P}_{Na}$	8×10^{-3} cm/s	sodium permeability constant
P'_K	1.2×10^{-3} cm/s	potassium permeability constant
$\bar{P}_P$	0.54×10^{-3} cm/s	nonspecific permeability constant
g_L	30.3 mmho/cm^2	leak conductance
V_L	0.026 mV	leak current equilibrium potential
$(Na)_o$	114.5 mM	external sodium concentration
$(Na)_i$	13.7 mM	internal sodium concentration
$(K)_o$	2.5 mM	external potassium concentration
$(K)_i$	120 mM	internal potassium concentration
F	96 514.0 C/g/mole	Faraday's constant
R	8.3144 J/K/mole	gas constant
T	295.18 K	absolute temperature.

Initial Conditions

$m(0) = 0.0005$
$h(0) = 0.8249$
$n(0) = 0.0268$
$p(0) = 0.0049$.

Acknowledgment

The author is indebted to Dr. C. P. Bean for providing many of the initial ideas from which this work was derived.

References

[1] J. D. Loeser, R. G. Black, and A. Christman, "Relief of pain by transcutaneous stimulation," *J. Neurosurg.*, vol. 42, p. 308, 1975.
[2] W. H. Sweet and J. G. Wepsic, "Treatment of chronic pain by stimulation of fibers of primary afferent neuron," *Trans. Amer. Neurol. Ass.*, vol. 93, p. 103, 1968.
[3] W. W. L. Glenn, J. H. Hagemann, A. Mauro, L. Eisenberg, S. Flanigan, and M. Harvard, "Electrical stimulation of excitable tissue by radio-frequency transmission," *Ann. Surg.*, vol. 160, p. 338, 1964.
[4] R. L. Waters, D. McNeal, and J. Perry, "Experimental correction of footdrop by electrical stimulation of the peroneal nerve," *J. Bone Joint Surg.*, vol. 57A, p. 1047, 1975.
[5] F. B. Simmons, "Electrical stimulation of the auditory nerve in man," *Arch. Otolaryngol.*, vol. 84, p. 2, 1966.
[6] G. S. Brindley and W. S. Lewin, "The sensations produced by electrical stimulation of the visual cortex," *J. Physiol.* (London), vol. 196, p. 479, 1968.
[7] R. FitzHugh, "Computation of saltatory conduction," *Biophys. J.*, vol. 2, p. 11, 1962.
[8] W. F. Pickard, "On the propagation of the nervous impulse down medullated and unmedullated fibers," *J. Theoret. Biol.*, vol. 11, p. 30, 1966.
[9] A. L. Hodgkin and A. F. Huxley, "A quantitative description of membrane current and its application to conduction and excitation in nerve," *J. Physiol.* (London), vol. 117, p. 500, 1952.
[10] L. Goldman and J. S. Albus, "Computation of impulse conduction in myelinated fibers: Theoretical basis of the velocity-diameter relation," *Biophys. J.*, vol. 8, p. 596, 1968.
[11] B. Frankenhaeuser and A. F. Huxley, "The action potential in the myelinated nerve fiber of *Xenopus Laevis* as computed on the basis of voltage clamp data," *J. Physiol.* (London), vol. 171, p. 302, 1964.
[12] W. A. H. Rushton, "The effect upon the threshold for nervous excitation of the length of nerve exposed, and the angle between current and nerve," *J. Physiol.* (London), vol. 63, p. 357, 1927.
[13] —, "A physical analysis of the relation between threshold and interpolar length in the electrical excitation of medullated nerve," *J. Physiol.* (London), vol. 82, p. 332, 1934.
[14] —, "Initiation of the propagated disturbance," *Proc. Roy. Soc. Ser. B.*, vol. 124, p. 210, 1937.
[15] P. G. Lale, "Muscular contraction by implanted stimulators," *Med. Biol. Eng.*, vol. 4, p. 319, 1966.
[16] D. Noble, "The relation of Rushton's 'liminal length' for excitation to the resting and active conductances of excitable cells," *J. Physiol.* (London), vol. 226, p. 573, 1972.
[17] J. J. Lussier and W. A. H. Rushton, "The excitability of a single fiber in a nerve trunk," *J. Physiol.* (London), vol. 117, p. 87, 1952.
[18] S. L. BeMent and J. B. Ranck, Jr., "A model for electrical stimulation of central myelinated fibers with monopolar electrode," *Expl. Neurol.*, vol. 24, p. 171, 1969.
[19] C. Abzug, M. Maeda, B. W. Peterson, and V. J. Wilson (with an Appendix by C. P. Bean), "Cervical branching of lumbar vestibulospinal axons," *J. Physiol.* (London), vol. 243, p. 499, 1974.
[20] W. A. H. Rushton, "A theory of the effects of fibre size in medullated nerve," *J. Physiol.* (London), vol. 115, p. 101, 1951.
[21] F. T. Dun, "The length and diameter of the node of ranvier," *IEEE Trans. Biomed. Eng.*, vol. BME-17, pp. 21-24, Jan. 1970.

[22] I. Tasaki, "New measurements of the capacity and the resistance of the myelin sheath and the nodal membrane of the isolated frog nerve fiber," *Amer. J. Physiol.*, vol. 181, p. 639, 1955.
[23] S. L. BeMent and J. B. Ranck, Jr., "A quantitative study of electrical stimulation of central myelinated fibers," *Expl. Neurol.*, vol. 24, p. 147, 1969.
[24] P. E. Crago, P. H. Peckham, J. T. Mortimer, and J. P. Van der Meulen, "The choice of pulse duration for chronic electrical stimulation via surface, nerve, and intramuscular electrodes," *Ann. Biomed. Eng.*, vol. 2, p. 252, 1974.
[25] R. Stampfli, "Bau und funktion isolierter markhaltiger nervenfasern," *Ergeb. Physiol.*, vol. 47, p. 70, 1952.
[26] F. A. Dodge and B. Frankenhaeuser, "Sodium currents in mylinated nerve," *J. Physiol.* (London), vol. 148, p. 188, 1959.
[27] J. B. Hursh, "Conduction velocity and diameter of nerve," *Amer. J. Physiol.*, vol. 127, p. 131, 1939.

The Characterization of Transcutaneous Stimulating Electrodes

KENNETH R. BRENNEN

Abstract—**A simple mathematical model of a transcutaneous stimulating electrode molded from conductive elastomer is used to predict the current density pattern produced by such electrodes. A general method has been developed to determine experimentally the current distribution produced by this class of electrodes. Preliminary experimental results are qualitatively in agreement with predictions made from the model. The experimental method for the determination of current spread yields a valid assessment of electrode performance independent of the accuracy of the mathematical model.**

I. Introduction

TRANSCUTANEOUS nerve stimulators apply controlled electrical pulses to the nervous system via electrodes placed on the skin. They have found broad application for the inhibition of pain. In a recent review Ray and Maurer listed the electrical and mechanical properties required of transcutaneous electrodes [1]. These include spread of current over at least 4 cm^2, to prevent skin irritation, and the flexibility to achieve conformability to the body.

Such electrodes are commonly molded from an elastomer, such as silicone rubber, loaded with carbon particles to provide conductance. Conformability is achieved by making the electrode thin. Useful carbon-loaded silicone rubbers typically have a minimum resistivity near 10 $\Omega \cdot$ cm.

A thin electrode may show an impedance which is not negligible compared to the impedance of the interface and tissue under it. This limits the spread of current over the electrode. Design of an electrode with the required conformability and current distributing properties becomes a compromise in electrode geometry and material properties. The frequency dependence of electrode performance must also be considered since the impedance between the electrode and subcutaneous tissue contains capacitance [2].

This article describes a method of modeling resistive electrodes along with an experimental method to determine the current spread produced by such systems. Fig. 1 shows the particular electrodes used in this study.

Manuscript received November 9, 1975; revised March 1, 1976.
The author is with the Neurological Division, Medtronic, Inc., Minneapolis, MN 55418.

II. Theory

At every point on a resistive electrode, the current can either flow outward through the body of the electrode or it can flow in a direction perpendicular to the plane of the electrode, crossing the interface and entering the underlying tissue. In fact, the current has components in both of these directions at every point. The relative impedances of the two pathways determine the magnitude ratio of the components. If we consider an electrode in the form of a long strip, the picture of the current distribution is as shown in Fig. 2. The current flowing down the electrode is constantly being diminished as it "loses" a component into the tissue. The rate of loss must be determined by the ratio of the resistance per unit length of the electrode to the resistance per unit area of the interface with the skin. Burton and Maurer support the assumption that the skin-electrode interface acts as a large two-dimensional impedance [2].

The physical situation described above is mathematically summarized in a family of equations known as cable equations. These well-studied equations generally describe current and energy losses from electrical systems consisting of a conductive core and an insulating but leaky sheath [3].

A solution to the cable equation for a resistive electrode in the form of a long strip is given by

$$j(x) = j_0 \exp(-X/L). \quad (1)$$

This equation describes the density j of current flowing into the skin at a distance x along the electrode (A/cm^2). The amplitude j_0 is given by

$$j_0 = -V_0/Z_i. \quad (2)$$

The impedance Z_i is the magnitude of the complex impedance of a unit area of the interface ($\Omega \cdot cm^2$), including the skin and underlying tissue. The latter may be treated as a small component of the areal impedance.